Journal of Applied Mechanics and Technical Physics, Vol. 44, No. 6, pp. 753–759, 2003

DIAGNOSTICS OF POWERFUL ELECTRON BEAMS USING TOTAL-ABSORPTION CALORIMETERS

A. P. Stepovik and D. V. Khmel'nitskii

UDC 536.6+539.12.04

The possibility of diagnosing an electron beam ejected into the atmosphere using total-absorption calorimeters is examined for the purpose of studying dynamic effects in materials irradiated in powerful electron accelerators. A diagram is given of the ring calorimeter used to measure energy fluence in IGUR-3 *and* ÉMIR-M *accelerators up to values of* $(2.0–2.5) \cdot 10^2$ J/cm^2. *The fraction of the incident electron energy absorbed in the calorimeter is calculated, the effect of the electron spectrum on the measurement results is shown, and heat-transfer problems are considered. It is established that measurement results can be used to determine the volume-averaged calorimeter temperature at the moment of termination of the electron pulse; this temperature is uniquely related to the electron energy absorbed in the calorimeter.*

Key words: *electron beams, powerful accelerator, absorbed energy, diagnostics, calorimeter.*

One method of loading materials by a short pulse of mechanical stress is exposure to a powerful electron beam (a duration of 10^{-8}–10^{-7} sec and a total beam current of tens of kiloamperes) [1]. Energy absorption in a time much smaller than the mechanical inertia of the material gives rise to thermoelastic stresses in it. This allows one to study spallation and to measure the thermodynamic and elastic parameters of materials [2, 3]. The relationship between the thermal pressure P that arises and the absorbed electron energy E_a is expressed by the well-known relation [4] $P = \Gamma d E_a$ (Γ is the Grüneisen coefficient of the material and d is its density).

The absorbed electron energy depends on the incident electron spectrum and energy fluence, which needs to be measured during pressure calculation. [The term particle energy fluence implies the ratio of the total energy (except for the rest energy) of all ionizing particles penetrating into the volume of an elementary sphere to the cross-sectional area of this sphere.] In powerful accelerators, the cross-sectional energy distribution of the electron beam ejected into the atmosphere [1] is insufficiently uniform; therefore, one needs to develop a diagnostic method that ensures minimum shadowing of the irradiated sample surface by the sensor (film dosimetry, foil calorimetry, etc.).

The energy fluence of the electron beam irradiating material samples was measured by calorimeters of two types: foil and total-absorption calorimeters [5]. Among the advantages of the calorimetric method are the possibility of recording the heating of the calorimeter after termination of the noise accompanying the operation of such devices [6] and the small dimensions of the sensor, which is important because of radiation inhomogeneity in the beam cross section.

Results of measurement using foil calorimeters are presented in more detail in [5]. These calorimeters allow measurements of the energy fluence of the electrons incident directly on a sample. However, foil calorimeter readings depend strongly on the sample material (from the data of our measurements, the readings can differ by a factor of 2 or 3) because the energy of the electrons reflected from the calorimeter contributes to the calorimeter heating.

In total-absorption calorimeters, the effect of reflected electrons is significantly diminished, but these calorimeters measure the energy fluence only in the neighborhood of a sample. The measurement error due to this factor is largely determined by the degree and shape of the energy distribution inhomogeneity in the electron beam cross section.

Institute of Engineering Physics, Snezhinsk 456770. Translated from Prikladnaya Mekhanika i Tekhnicheskaya Fizika, Vol. 44, No. 6, pp. 4–11, November–December, 2003. Original article submitted July 23, 2002; revision submitted January 4, 2003.

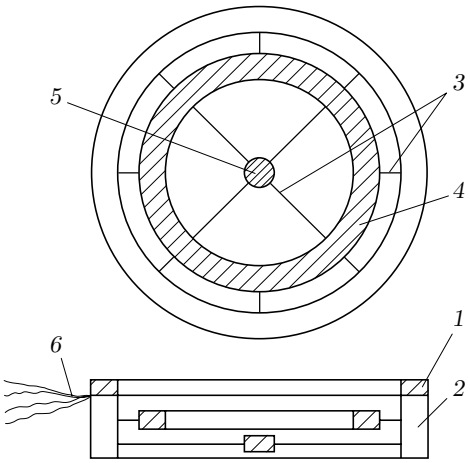

Fig. 1. Diagram of the ring calorimeter: steel ring (1), casing (2), guys (3), ring calorimeter (4), central calorimeter (5), and thermocouples (6).

In the development of diagnostic procedure using the indicated calorimeters on IGUR-3 and ÉMIR-M facilities [1], local copper and steel calorimeters 2–3 mm thick and 3.5–6 mm in diameter were employed. Thermocouples were sealed in the calorimeter body from the rear side (relative to the electron flow) and were then glued to a plate of laminate (which has the highest resistance to the action of electrons compared to the other organic materials). For an energy fluence of up to 10 J/cm^2, such calorimeters can be used repeatedly. However, for large values of this parameter (due to thermal shock), the calorimeters separated from the plate, and under severe heating, the thermocouples sealed out and failed. As a result, the examined range of dynamic stress amplitudes narrowed (to 100 MPa in aluminum).

To increase the resistance of the calorimeters to the action of powerful pulsed electron beams, we designed the setup shown schematically in Fig. 1. The grounded ring is intended to protect the casing from the action of electrons. The guys were manufactured from a steel wire of 0.4 mm diameter. One thermocouple is embedded in the central calorimeter, and four thermocouples are embedded (uniformly over the circumference) in the ring calorimeter. For a sample of 50–60 mm diameter, the sample shadowing, determined by the surface area of the central calorimeter of 6 mm diameter, was insignificant. The thermocouples are placed in a groove in the casing and are led out as a braid. In experiments with samples of 10–15 mm diameter, several ring calorimeters (one calorimeter for each sample) were housed in the casing and central calorimeters were absent.

Calorimeter temperature variation was recorded by self-recording ÉPP-09M3 potentiometers or N-37 direct current milliampermeters with an I-37 amplifier. This instrumentation was chosen because of its stability (due to slow response) to the nano- and microsecond electrical noise occurring in the facilities used. In this case, the thermal e.m.f. of the thermocouples was measured in approximately 1 sec after irradiation by electrons.

In using the designed setup to diagnose an electron beam, one needs to estimate the thermal characteristics of the calorimeter and the effect of the electron spectrum and irradiation conditions on measurement results. In this case, it is necessary to take into account the following circumstances. First, some of the electrons incident on the calorimeter are reflected from its surface, some electrons leaves the calorimeter through its lateral surfaces due to scattering, and, finally, the electron energy is partly expended in photon radiation during their deceleration in the material. As a result, the energy of the incident electrons is not entirely expended in heating the calorimeter. Second, since the calorimeter is in the atmosphere, it is necessary to take into account the calorimeter temperature variation due to cooling and redistribution of the absorbed energy over the volume. To correctly take into account the effect of the above-mentioned factors on the accuracy of electron beam diagnostics, we consider them in more detail.

To determine the fraction of electron energy absorbed in the calorimeter material, we calculated electron propagation in iron bodies of different shapes ($d_{\mathrm{Fe}} = 7.8 \cdot 10^3$ g/m^3) using the Monte Carlo technique with the MCNP4A program. The bodies were rings and disks made of St. 3 steel of thickness $h = 0.3$ cm, including bodies of the same dimensions as those of the calorimeters (disk radius $R_0 = 0.3$ cm, ring inner radii $R_1 = 2.0$ and 2.25 cm and outer radii $R_1 = 2.60$ and 2.85 cm). The electron source was a plane parallel to the end surface of the body

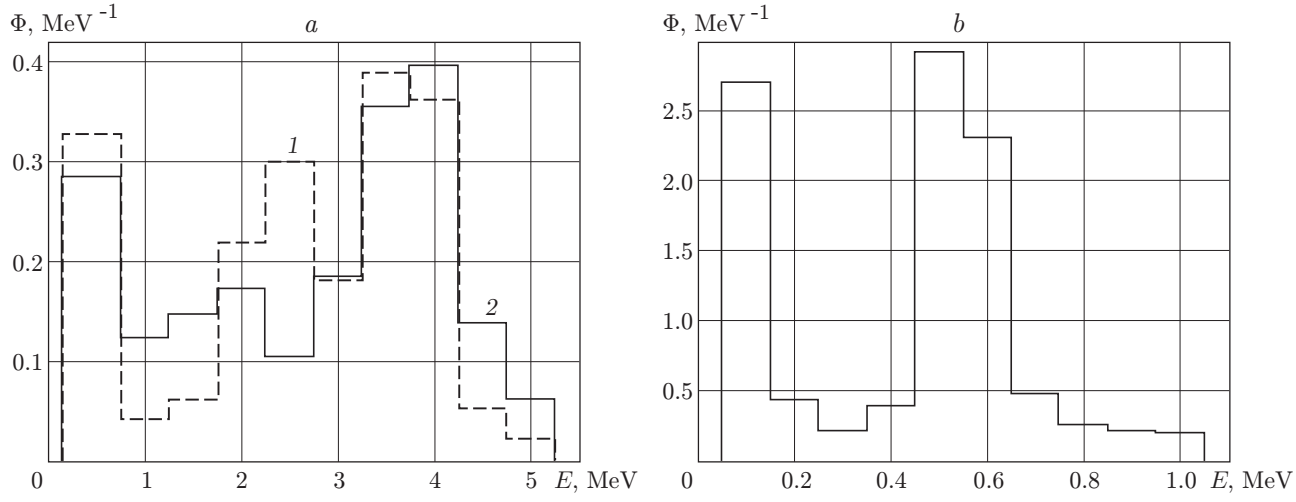

Fig. 2. Electron energy spectra for $E_{\max} = 5.2$ (a) and 1.05 MeV (b): spectrum 1 refers to $t' \approx$ 90 nsec and $\langle E \rangle = 2.59$ MeV and spectrum 2 refers to $t' \approx 25$ nsec and $\langle E \rangle = 2.68$ MeV.

TABLE 1

Calculation version	Sizes, cm	$E_{\max}$, MeV	$\langle E \rangle$, MeV	$E_{\rm a}$, MeV	$E_{\rm e}$, MeV	$E_{\rm p}$, MeV	$E_{\rm e1}$, MeV	$E_{\rm e2}$, MeV	χ
No. 1	$R_0 = 5$	5.2	2.59 (0.5)	2.32 (0.6)	0.164 (3)	0.100 (3)	$2.3 \cdot 10^{-3}$ (22)	0.021 (10)	0.898
No. 2	$R_0 = 5$	5.2	2.68 (0.5)	2.40 (0.6)	0.166 (3)	0.111 (3)	$6.3 \cdot 10^{-3}$ (13)	0.024 (10)	0.897
No. 3	$R_0 = 0.5$	5.2	2.68 (0.5)	2.18 (0.6)	0.390 (2)	0.110 (3)	$5.6 \cdot 10^{-3}$ (14)	0.262 (3)	0.813
No. 4	$R_0 = 0.3$	5,2	2,68 (0,5)	2,02 (0.6)	0.550 (2)	0.108 (3)	$4.8 \cdot 10^{-3}$ (16)	0.433 (3)	0.755
No. 5	$R_1 = 2.0$, $R_2 = 2.6$	5.2	2.68 (0.5)	2.22 (0.6)	0.355 (2)	0.110 (3)	$6.0 \cdot 10^{-3}$ (16)	0.231 (3)	0.827
No. 6	$R_1 = 2.25$, $R_2 = 2.85$	5.2	2.68 (0.5)	2.22 (0.6)	0.355 (2)	0.111 (3)	$5.4 \cdot 10^{-3}$ (15)	0.231 (3)	0.827
No. 7	$R_0 = 0.3$	1.05	0.431 (0.2)	0.358 (0.5)	$7.03 \cdot 10^{-2}$ (0.7)	$2.74 \cdot 10^{-3}$ (3)	0	$9.94 \cdot 10^{-3}$ (2)	0.831
No. 8	$R_1 = 2.0$, $R_2 = 2.6$	1.05	0.431 (0.2)	0.363 (0.5)	$6.59 \cdot 10^{-2}$ (0.7)	$2.58 \cdot 10^{-3}$ (3)	0	$5.22 \cdot 10^{-3}$ (3)	0.842

Note. Statistical errors of calculation results are given in parentheses. (1σ, %).

and located at 100 cm from this surface. The direction of electron escape coincided with the normal direction to the body surface. Figure 2 shows three electron energy spectra $\Phi(E)$: two hard spectra with identical maximal energies $E_{\max} = 5.2$ MeV for different operating regimes of the IGUR-3 facility (pulse duration $t' \approx 90$ and 25 nsec) [1] and a softer spectrum with $E_{\max} = 1.05$ MeV. Collective transfer of electrons and photons was taken into account.

Results of the calculations are given in Table 1, where $\langle E \rangle$ is the average beam electron energy, $E_{\rm a}$ is the energy of the electrons and photons absorbed in the calorimeter, $E_{\rm e}$ and $E_{\rm p}$ are the energies of electrons and photons that escape from the system, including $E_{\rm e1}$ and $E_{\rm e2}$, the energies of electrons that escape from the system through the other end surface and the lateral surfaces, respectively, and $\chi = E_{\rm a}/\langle E \rangle$ is the fraction of the energy absorbed in the calorimeter. The given results are normalized per one electron of the source.

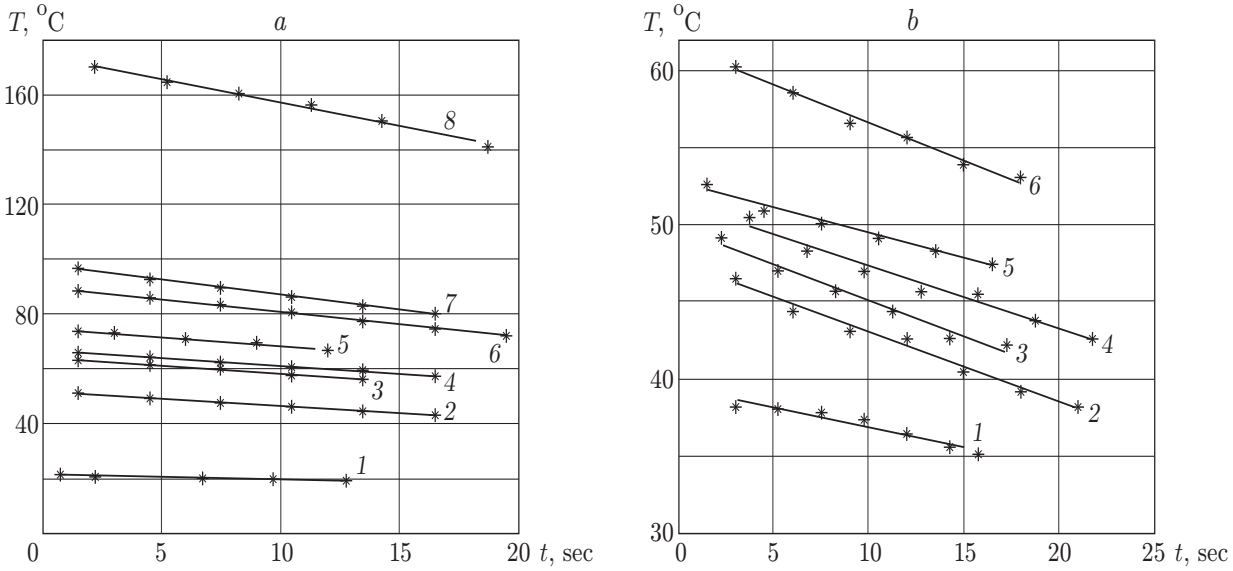

Fig. 3. Thermocouple temperature versus time for the central (a) and ring (b) calorimeters: the points are experimental data, the curves are least-squares fittings (curve numbers correspond to the numbers in Table 2).

In calculation version Nos. 1 and 2, we considered a calorimeter shaped like a disk of radius $R_0 = 5$ cm for two hard electron spectra (Fig. 2a). For both electron spectra, the fraction of the energy absorbed in the calorimeter were identical. This implies that the value of χ is determined primarily by the average energy of incident electrons and depends weakly on the shape of the energy spectrum.

The calculation results show that the shape of the calorimeter has a significant effect on the electron energy absorption in it: the values of χ vary from 0.9 to 0.75 (Table 1). This is due primarily to an increase in the fraction of electrons that escaped through the lateral surfaces of the calorimeter as its cross-sectional dimension decreases. The fraction of the beam energy carried away by electrons that passed through the calorimeter is very low (less than 0.5% $\langle E \rangle$). The energy of photons that escaped from the calorimeter does not depend on the cross-sectional dimension of the calorimeter and is approximately 3% of the initial electron energy. For both types of ring calorimeter, the calculation results coincide within the error despite the difference in the outer and inner radii (for an identical width of the ring $R_2 - R_1$).

In version Nos. 7 and 8, the average energy of the source electrons (Fig. 2b) was approximately six times lower than that for the first two spectra (Fig. 2a); therefore, the electron free path in the calorimeter and the energy loss by radiation are smaller and, hence, the fraction of the absorbed energy is higher.

To take into account the effect of electron scattering in air on the energy absorbed in the calorimeter, we performed calculations modeling the passage of unidirectional electrons through an air layer of different thicknesses (3 and 30 cm) between the source and the ring calorimeter. The results showed that the value of χ did not change within the statistical error ($1\sigma \approx 1$–2%).

To determine the calorimeter temperature T at the thermocouple location from the measured thermal e.m.f., we used an approximating polynomial [7]. Figure 3 shows curves of calorimeter temperature versus time during cooling after exposure to an electron beam. The coefficients of the approximating polynomial of the form $T = a_0 - a_1 t$ for each of these dependences and the maximum heating of the calorimeters T_1 (the first measured temperature value) are given in Table 2. From the data given in Fig. 3, it follows that for the recording time (1–20 sec), the dependence $T(t)$ can be considered linear with sufficient accuracy (especially for the central calorimeter).

Let us determine the relationship of the experimental constants a_0 and a_1 with the calorimeter heating and its thermal characteristics. The change in the calorimeter temperature after electron-beam irradiation is due to heat transfer to the ambient air by free convection and thermal radiation. The effect of thermal conduction through the calorimeter mounting elements on the process of calorimeter cooling can be ignored because the steel wire has a small diameter and is heated simultaneously with the calorimeter by the electron beam.

TABLE 2

Central calorimeter				Ring calorimeter			
Curve number in Fig. 3a	T_1,°C	a_0	a_1	Curve number in Fig. 3b	T_1,°C	a_0	a_1
1	21.1	20.9	0.170	1	38.2	39.4	0.253
2	50.9	51.3	0.512	2	46.55	47.5	0.454
3	62.9	63.8	0.567	3	49.2	49.8	0.470
4	63.4	66.3	0.574	4	50.5	51.4	0.406
5	73.2	74.5	0.631	5	52.6	52.7	0.329
6	88.1	89.7	0.916	6	60.3	61.5	0.487
7	96.4	97.7	1.110				
8	170.4	174.2	1.730				

Since the change in the calorimeter temperature under cooling is insignificant over the measurement time, the expression for heat exchange on the calorimeter surface can be written as

$$f = \alpha(T - T_\infty) + \sigma_s \varepsilon (T^4 - T_\infty^4) = \alpha^*(T)(T - T_\infty) \approx \alpha^*(T_1)(T - T_\infty),$$

where f is the heat flux density, T_∞ is the ambient temperature, α is the coefficient of heat release by free convection of air, $\sigma_s = 5.67 \cdot 10^{-8}$ W/(m$^2 \cdot$K^4) is the Stefan–Boltzmann constant, and ε is the emissivity factor of the calorimeter surface ($\varepsilon \approx 0.7$ [8]).

From consideration of the one-dimensional problem of cooling of a body on whose surface there is heat exchange with the ambient medium, it follows that the characteristic time of temperature variation is determined by the quantity $\tau_0 = \tau/x_1^2$, where $\tau = h^2 C d/\lambda$ (h is the size of the body, λ is the thermal conductivity of the material, C is its specific heat, d is the density) and x_1 is the least root of the equation $x \tan x = L = \alpha^* h/\lambda$ [8]. Under the conditions considered ($h = 0.3$ cm) even for $E \approx 200$ J/cm^2, which corresponds to a calorimeter heating of approximately 180°C, taking into account heat release by free convection [$\alpha^* < 100$ W/(m$^2 \cdot$K)], we have $L < 5 \cdot 10^{-3} \ll 1$ [for iron, $\lambda = 57$ W/(m$\cdot$K] at $T = 100$°C [9]) and $\tau_0 \simeq Cdh/\alpha \gg \tau$. The characteristic time of variation in the average calorimeter temperature τ_0 is much larger than the time of heat propagation within the calorimeter τ. Therefore, for calorimeter cooling at times $t > \tau$, the temperature distribution over the calorimeter volume can be considered uniform. Then, integration of the heat-conduction equation over the calorimeter volume subject to the boundary conditions leads to the equation

$$C(T) V d \frac{dT}{dt} + \alpha^*(T) S_\text{s} (T - T_\infty) = 0 \tag{1}$$

with the initial condition $T|_{t=0} = \langle T_0 \rangle$, where $\langle T_0 \rangle$ is the average calorimeter temperature after irradiation. In (1), V is the calorimeter volume and S_s is the total calorimeter surface area on which heat exchange occurs.

Since for calorimeter cooling, the experimental temperature–time dependences are linear, we seek a solution of Eq. (1) in an approximation linear in time:

$$T(t) = \langle T_0 \rangle - (\langle T_0 \rangle - T_\infty) t/\tau_0, \qquad \tau_0 = C(\langle T_0 \rangle) V d/(\alpha^*(\langle T_0 \rangle) S_\text{s}). \tag{2}$$

We note that the above expression for the calorimeter considered is valid under the condition $t/\tau_0 \ll 1$, which, in turn, holds at $t < 40$ sec (for iron, $C = 462$ J/(kg$\cdot$K) at $T = 20$°C [9]). Comparing the form of the first expression in (2) with the polynomial approximating experimental data, we obtain $a_0 = \langle T_0 \rangle$. Thus, extrapolating the experimental dependences at the moment of termination of the electron pulse, we obtain the temperature averaged over the calorimeter volume at this time.

Since the electron pulse duration is much smaller than the characteristic time of heat propagation in the calorimeter ($\tau \approx 0.1$ sec), it can be assumed that the heat release in the calorimeter volume occurs simultaneously and the temperature at each point is determined by the absorbed particle energy. After a lapse of time $t \geqslant \tau$, the temperature becomes equal to the temperature-averaged over the calorimeter volume. We note that the calorimeter heat losses by radiation within this time due to overheating of the irradiated surface (calculations show that the heating of the regions adjacent to the surface is less than twice the average heating of the calorimeter) are

approximately 0.1% of the electron energy incident on the calorimeter. Then, with allowance for the temperature dependence of the specific heat of iron, the relation between the calorimeter temperature at the moment of pulse termination $\langle T_0 \rangle$ and the particle energy absorbed in the calorimeter during the pulse E_a is defined by the relation

$$Vd \int_{T_\infty}^{\langle T_0 \rangle} C(T)\, dT = E_a = \chi W S,$$

where W is the energy fluence of the beam electrons (which is constant on the irradiated calorimeter surface S).

Using the data of [10] on the temperature dependence of the specific heat of iron in the range from 250 to 600 K, the quantity W can be expressed in terms of known values of T_∞ and $\langle T_0 \rangle = a_0$ as follows:

$$W = hd(H(\langle T_0 \rangle) - H(T_\infty))/\chi,$$

$$H(T) = \int C(T)\, dT = \begin{cases} 422T + 67(T-250)^2/300, & 250 \leqslant T \leqslant 400, \\ 489T + 85(T-400)^2/400, & 400 \leqslant T \leqslant 600 \end{cases}$$

(h is the thickness of the calorimeter).

The average value α^* can be estimated using experimental data on cooling of the calorimeters (Fig. 3). Indeed, the form of expressions (2) implies

$$\alpha^*(T_1) = a_1 C(\langle T_0 \rangle) Vd/((\langle T_0 \rangle - T_\infty) S_s).$$

Among the quantities included in the given expression, the ambient temperature is an unknown; in the experiments, it was 17–22°C. The coefficients α^* for each measurement at $T_\infty = 17$ and 22°C were found taking into account the dimensions of the central and ring calorimeters and the measured values of a_1 and $\langle T_0 \rangle = a_0$ (Table 2). From the results of calculations for different measurements, we determined the average value and standard deviation: $\alpha^* = (31.8 \pm 6.8)$ W/(m$^2 \cdot$K). The obtained value ensures satisfaction of the condition $L \ll 1$ for the calorimeter considered, which, in turn, allows the use of this calorimeter and the procedure described above to determine the magnitude of the electron beam energy fluence from calorimeter temperature measurements during calorimeter cooling.

The proposed calorimeter design, repeatedly used in experiments (see [2, 11]), allow measurements of electron energy fluence on IGUR-3 and ÉMIR-M facilities up to $(2.0\text{–}2.5) \cdot 10^2$ J/cm^2 (this corresponds to pressures of about 2 GPa in aluminum). This has made it possible to explore spallation in copper and aluminum alloys, to measure the Grüneisen coefficient of pyrocarbon, etc. The design turned out to be convenient in operation because it is resistant to the action of an electron beam and can be used as a separate unit. It can be mounted in a device for irradiating samples, replaced in the case of damage due to reuse near limiting values of energy fluence, etc. It is possible to estimate the applicability limit for the given calorimeter design at different irradiation levels. The limiting value of W is determined by spallation of the material of the calorimeter face (initial stage of damage in a single exposure to an electron beam) and depends on a number of parameters: the spectrum and duration of the electron beam of the facility, the thermodynamic parameters of the calorimeter material, etc. For a calorimeter made of St. 3 steel and the facilities used, the limiting value of the electron energy fluence is approximately 300 J/cm^2, and for titanium or carbon calorimeters, it is larger.

REFERENCES

1. V. S. Diyankov, V. P. Kovalev, A. I. Kormilitsyn, et al., "Experimental facilities for radiation studies at the Research Institute of Technical Physics," *Fiz. Metal. Metalloved.*, **81**, No. 2, 119–123 (1996).
2. A. P. Stepovik, "The Grüneisen coefficient of UPV-1 pyrolitic carbon," *J. Appl. Mech. Tech. Phys.*, **4**, 611–612 (1992).
3. R. B. Oswald, D. R. Schallhorn, H. A. Eisen, and F. B. McLeon, "Dynamic response of solids exposed to a pulsed-electron-beam," *Appl. Phys. Lett.*, **13**, No. 8, 279–281 (1968).
4. Ya. B. Zel'dovich and Yu. P. Raizer, *Physics of Shock Waves and High-Temperature Hydrodynamic Phenomena* [in Russian], Nauka, Moscow (1966).
5. A. P. Stepovik, "Methodical features of measurement of mechanical stresses in materials exposed to powerful electron beams" in: *Questions of Atomic Science and Engineering*, *Ser. Physics of Radiation Actions on Radioelectronic Instrumentation*, Nos. 3/4 (1999), pp. 132–138.

6. A. P. Stepovik and A. I. Kormilitsyn, "Spatial distribution of the electromagnetic field of an IGUR-3 facility near an accelerating tube," in: *Questions of Atomic Science and Engineering, Ser. Physics of Radiation Actions on Radioelectronic Instrumentation*, Nos. 1/3 (1996), pp. 203–206.
7. I. L. Rogel'berg and V. M. Beilin, *Alloys for Thermocouples, Handbook* [in Russian], Metallurgiya, Moscow (1983).
8. G. Karslow and D. Eger, *Thermal Conductivity of Solids* [Russian translation], Nauka, Moscow (1964).
9. M. A. Mikheev and I. M. Mikheeva, *Fundamentals of Heat Transfer* [in Russian], Énergiya, Moscow (1977).
10. I. S. Grigor'ev amd E. Z. Meilikhov (eds.), *Physical Quantities: Handbook* [in Russian], Énergoatomizdat, Moscow (1991).
11. A. P. Stepovik, "Effect of rolling conditions on the nature of damage of copper and aluminum alloys under subsequent dynamic loading," *Fiz. Metal. Metalloved.*, **84**, No. 6, 104–108 (1997).